DOE/MC/29061-96/C0663

CONF-9510109--42

Combustion Modeling in Advanced Gas Turbine Systems

Author:

L. Douglas Smoot
Thomas H. Fletcher
Stephen K. Kramer
Paul O. Hedman
B. Scott Brewster

Contractor:

South Carolina Energy Research and Development Center
Clemson University
Clemson, SC 29634

Contract Number:

DE-FC21-92MC29061
Subcontract No. 93-01-SR014

Conference Title:

Advanced Turbine Systems Annual Program Review

Conference Location:

Morgantown, West Virginia

Conference Dates:

October 17-19, 1995

Conference Sponsor:

U.S. Department of Energy, Office of Power Systems Technology,
Morgantown Energy Technology Center

Contracting Officer Representative (COR):

Norman Holcombe

Disclaimer

P8 Combustion Modeling in Advanced Gas Turbine Systems

L. Douglas Smoot (lds@byu.edu; 801-378-8930)
Paul O. Hedman (hedman@byu.edu; 801-378-6238)
Thomas H. Fletcher (tom@harvey.et.byu.edu; 801-378-6236)
B. Scott Brewster (brewster@guitar.et.byu.edu; 801-378-6240)
Stephen K. Kramer (kramer@bones.et.byu.edu; 801-378-4548)
Advanced Combustion Engineering Research Center
45 Crabtree Building, Brigham Young University
Provo, UT 84602

Introduction

The goal of the U.S. Department of Energy's Advanced Turbine Systems (ATS) program is to help develop and commercialize ultra-high efficiency, environmentally superior, and cost competitive gas turbine systems for base-load applications in the utility, independent power producer, and industrial markets. Combustion modeling, including emission characteristics, has been identified as a needed, high-priority technology by key professionals in the gas turbine industry.

Objective

The primary objective of the four year ATS program at this center is to develop a comprehensive combustion model for advanced gas turbine combustion systems using natural gas fuel with consideration of coal gasification or biomass fuels.

Approach

Three tasks have been undertaken to achieve the overall objective of this program.

Research sponsored by the U.S. Department of Energy's Morgantown Energy Technology Center, under cooperative agreement No. DE-FC21-92MC29061 with South Carolina Energy Research and Development Center, 386-2 College Avenue, Clemson University, Clemson, SC 29634-5181; telefax: 803-656-1429, subcontract 93-01-SR014 with Advanced Combustion Engineering Research Center, Brigham Young University, 45 CTB, BYU, Provo, UT 84602; telefax: 801-378-3831.

The first task is to improve and validate various submodels needed to accurately predict various aspects of the gas turbine combustion process. Of particular emphasis are submodels for predicting carbon monoxide and nitrogen oxides, particularly at the higher temperatures and pressures proposed for advanced turbine systems. Ongoing improvements in existing submodels such as turbulence, finite-rate chemistry, and pollutant emissions are also being considered for addition to the 3-D code. These submodels will be validated by data obtained with advanced diagnostic systems from the LSGTC.

The second task is to refine the BYU/ACERC 3-D code (PCGC-3) for application to gas turbine combustors and implement proven submodels into the gas turbine model. Refinements and submodels will also be available for incorporation into other prominent computational fluid dynamics (CFD) platforms such as those from Fluent, a commercial developer of CFD codes.

The third task is to interact extensively with industrial and university organizations with strong gas turbine interest. An ACERC/ATS technical advisory committee (TAC) composed of prominent industrial organizations with specific interest in utility and industrial gas turbine manufacture and application has been formed. The TAC provides direction and support of this research program. Concerns particular to the industry are being addressed, and results will be provided to participating industrial members.

Results

Key accomplishments of the past year are described below.

Task 1 - Submodel Development

The first task is to improve and validate various submodels needed to accurately predict various aspects of the gas turbine combustion process.

1.1 - Code Evaluation. The objective of this subtask was to evaluate the existing PCGC-3 code by comparing model results to local measurements from the BYU/ACERC laboratory-scale gas turbine combustor (LSGTC). Variables of interest included local gas velocities and temperatures. Key model needs were identified through this effort. Work on this subtask was completed during the first year of the study.

1.2 - Fundamental Experiments. The objective of this subtask is to conduct key experiments in the LSGTC to provide needed data for PCGC-3 and submodel evaluation. Measurements include: 1) gas temperatures and concentrations of CO, CO_2, O_2, and N_2 using coherent anti-Stokes Raman spectroscopy (CARS), 2) velocity components using laser Doppler anemometry (LDA), 3) presence of OH, CH, CO, NO, NO_2 and possibly N_2O using planar, laser-induced fluorescence (PLIF), and 4) flame and flow structure using digitized images from film or video cameras.

Dual-Stokes CARS Measurements. The dual-Stokes CARS system which is designed to simultaneously measure near-instantaneous concentrations of CO, CO_2, N_2, and O_2, was reduced in size to accommodate the setup of other laser-based diagnostic techniques. The CARS optical system has been optimized and a full gas temperature map of the LSGTC was measured. Example spectra at two locations are presented in Figure 1.

Figure 1a is near the burner exit (z = 1.0 cm, r = 0.9 cm) and has an estimated mean temperature of 800 K. The mean spectrum at this location shows that small amounts of O_2 are present along with CO_2. At this location at the onset of the reaction zone, unburned fuel and products will co-exist. Five centimeters further along the reaction zone, the smaller O_2 signal and a relatively larger CO_2 signal indicate the progress of the reaction (Figure 1b, z = 6.0 cm and r = 3.3 cm). The mean temperature for this location is approximately 1400 K.

A program (CARS.F) was obtained from Sandia National Laboratories in order to extract temperature and specie concentrations from these spectra. However, this program only reduces one spectrum at a time. Accurate representation of the statistical properties of the turbulent flame being studied used five hundred laser shots from each location. Therefore, an additional program was written and linked to CARS.F to extract and reduce single laser shots sequentially obtained from the file containing all five hundred. This shell program also subtracts out the background signal and normalizes the spectrum against the non-resident signal. The shell program was validated with signals obtained in known temperature environments. Problems that have been found with the manner the Sandia CARS.F program handles data are being resolved.

LDA Measurements. Laser Doppler Anemometry measurements of axial, radial, and tangential velocities were obtained on the LSGTC for an air flow of 500 slpm at $\phi = 1.1$, $\phi = 1.0$, $\phi = 0.8$, and $\phi = 0.65$ with the medium swirl (MS) configuration. Recirculation zones were identified as well as other flow features. Mean flow velocities and root-mean-square velocities were determined.

Figure 2 presents some example velocity PDFs generated from the LDA data obtained during this study. These PDFs are important to code development and verification. Currently, PCGC-3 assumes a scalar PDF shape, such as Gaussian, for the entire flow field. Figure 2 shows velocity PDFs for the ATS-MS burner at $\phi = 0.65$. The PDFs presented in this figure were calculated from velocity measurements taken at an axial location of 5 mm above the injector and at radial locations of 12 mm, 15 mm and 18 mm. Each column of axial, radial and tangential velocity PDFs corresponds to the

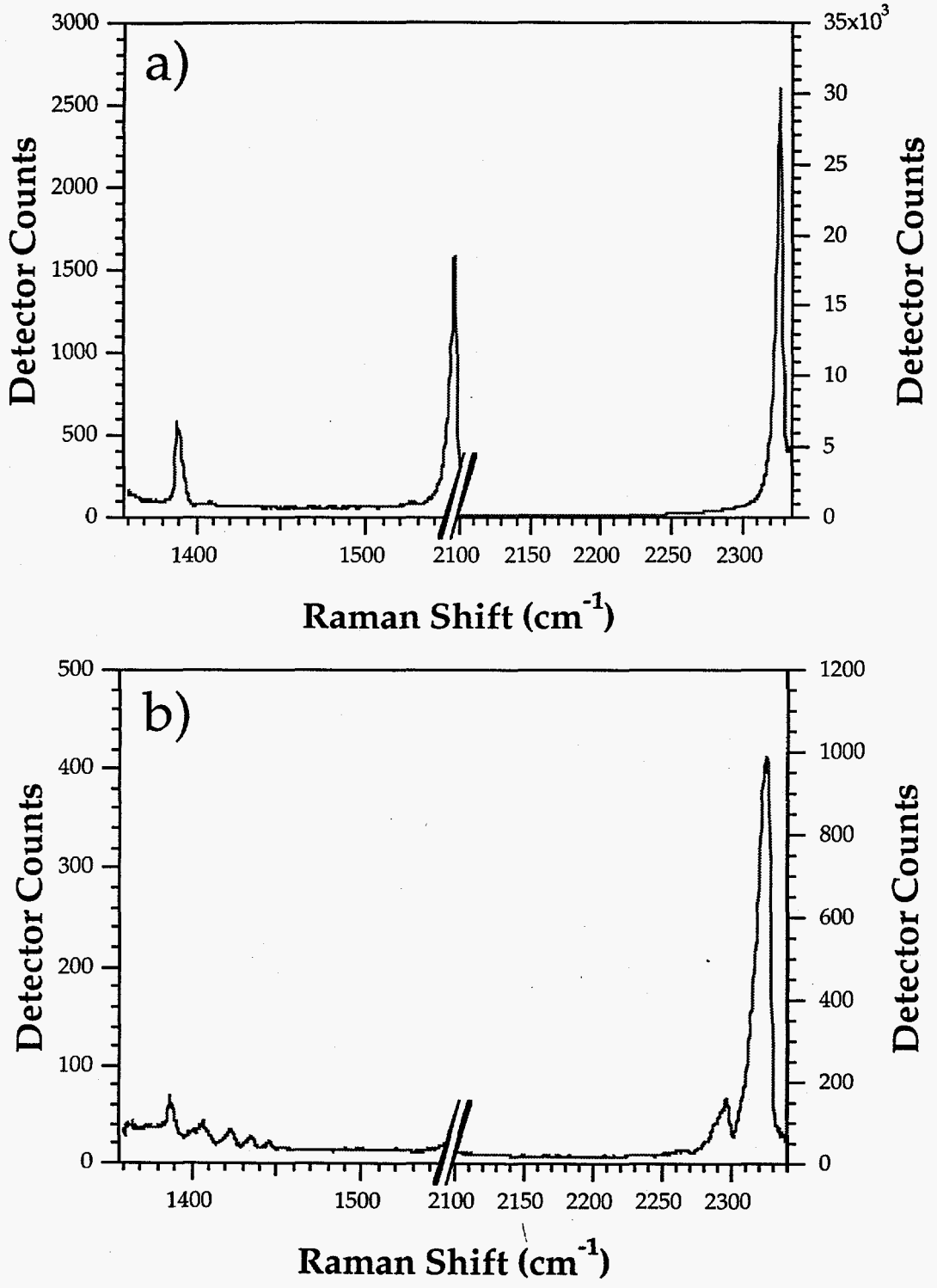

Figure 1. Sample averaged spectra in the LSGTC at a) z= 1.0 cm, r = 0.9 cm and b) z = 6.0 cm and r = 3.3 cm.

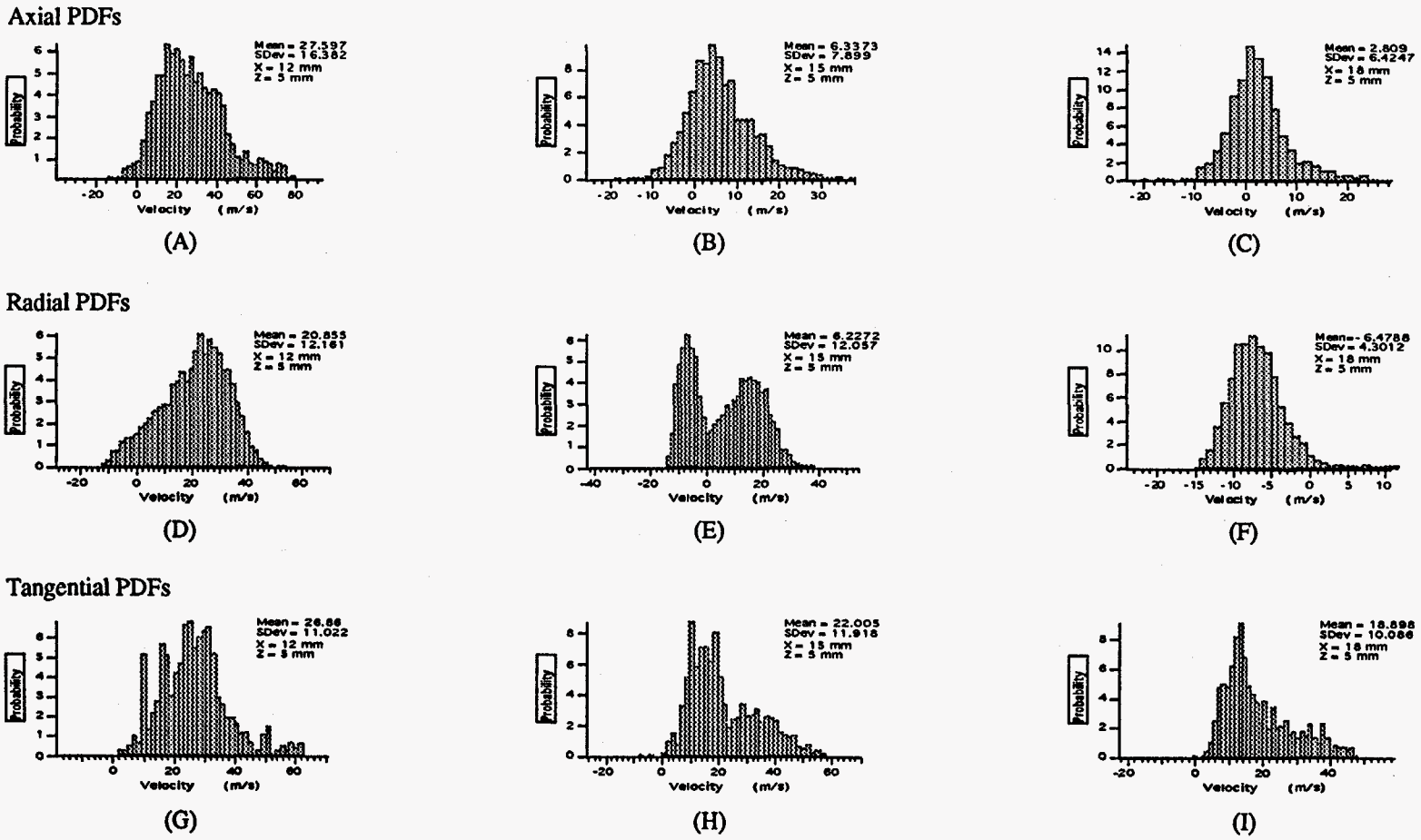

Figure 2. Axial, radial and tangential velocity pdfs at radial locations of 12 mm, 15 mm, and 18 mm, and an axial location of 5 mm downstream of the injector. ATS-MS burner, premixed natural gas/air, air flow rate of 500 slpm, $\phi = 0.65$.

same radial location in the burner. The axial velocity distribution, Figures 2A-2C, remained fairly Gaussian as one moved from inside the vortex, through the shear zone and into the surrounding outside gases. The large decrease in mean velocity caused by momentum dissipation in the shear zone is readily observed. The radial velocity PDFs, Figures 2D-2F, show the interaction of the gases forced out by the vortex and those being recirculated in the lower corners of the combustor. Figure 2E, which shows the velocity PDF at the shear layer, has a bimodal distribution with one peak occurring near the radial velocity value inside the vortex, and the other peak being near the velocity value found in the recirculation zone. The tangential velocity PDFs , Figures 2G-2I, show a similar trend to the radial velocity PDFs . The velocity PDF in the shear zone, Figure 2H, has a bimodal distribution with peaks near the tangential velocity values measured to either side of the shear zone.

Figure 3 shows an example of an axial-radial $\overline{u'v'}$ and axial-tangential $\overline{u'w'}$ Reynolds stress contour map of the ATS-MS burner at ϕ = 0.65. Many modeling approaches assume that the Reynolds stress is isotropic. From Figure 3, it is apparent that the Reynolds stresses are not isotropic for this system. The contour shapes, locations, and magnitudes differ significantly for the axial-radial (Figure 3A) and the axial-tangential (Figure 3B) Reynolds stresses. The Reynolds stress magnitudes for $\overline{u'v'}$ range from -5 to 50 m^2/s^2, while those for $\overline{u'w'}$ range only from -5 to 25 m^2/s^2. The largest Reynolds stresses occur in the region along the vortex wall, which indicates that there are high turbulence levels and large momentum transport at the boundary between the vortex and the gases in the burner. This observation is consistent with the conclusions drawn from the mean and RMS velocity contours, which showed high RMS velocity values and rapid decay of the mean velocity at the vortex wall due to shearing between the high velocity swirling gases from the injector and the lower velocity gases in the burner.

Planar Laser Induced Fluorescence (PLIF) of CH radicals. PLIF images of CH have been successfully acquired in a natural gas, premixed Bunsen burner flame. CH is an excellent marker of the flame zone and can actually be observed by the eye as part of the bright, inner blue chemiluminescent cone. Previous fluorescent studies used OH to mark the flame zone; however, OH is known to persist longer in the flame. CH is a better flame zone marker due to its very high reactivity and because it is also implicated in the formation of prompt NO_x.

Excitation of CH occurs at a wavelength near 387 nm. This light is generated by wave mixing the fundamental of a Nd:YAG DCR-2A laser(1064 nm) with the output of a tunable dye laser using Rhodamine 640 dye. The Nd:YAG pumps the tunable dye laser with frequency doubled 1064 nm light, and the residual is used for mixing in the WEX (Wave Length Extender). The total power of the 387 nm laser light is 14 mJ/pulse with a 10 ns pulse width. The laser light is optically formed into a sheet and passed through the flame as shown in Figure 4. Fluorescence at 431 nm is captured by an Intensified Charge Coupled Device (ICCD) using a Nikon 50 mm/f 1.2 lens and a GG-420 long-pass filter. The images are downloaded to a computer for further analysis. Figure 4 also shows four instantaneous images of the fluorescence emitted from the CH radical.

1.3 - Submodel Improvements. The objective of this subtask is to improve the submodels in the code using available technology and advances from this study, from other ACERC researchers under independent funding, and from the literature, in order to provide increased agreement with the key experiments identified in Subtask 1.2. Specific submodels being considered include finite-rate chemistry, NO_x formation at high pressures in fuel-lean systems, and CO/CO_2 non-equilibrium.

Evaluation of Reduced Mechanisms. A comprehensive study was conducted to select and evaluate potential reduced mechanisms of methane combustion for use in comprehensive premixed turbulent combustion codes. The two most promising mechanisms were by Seshadri and Peters (Chen and Dibble, 1991) and by

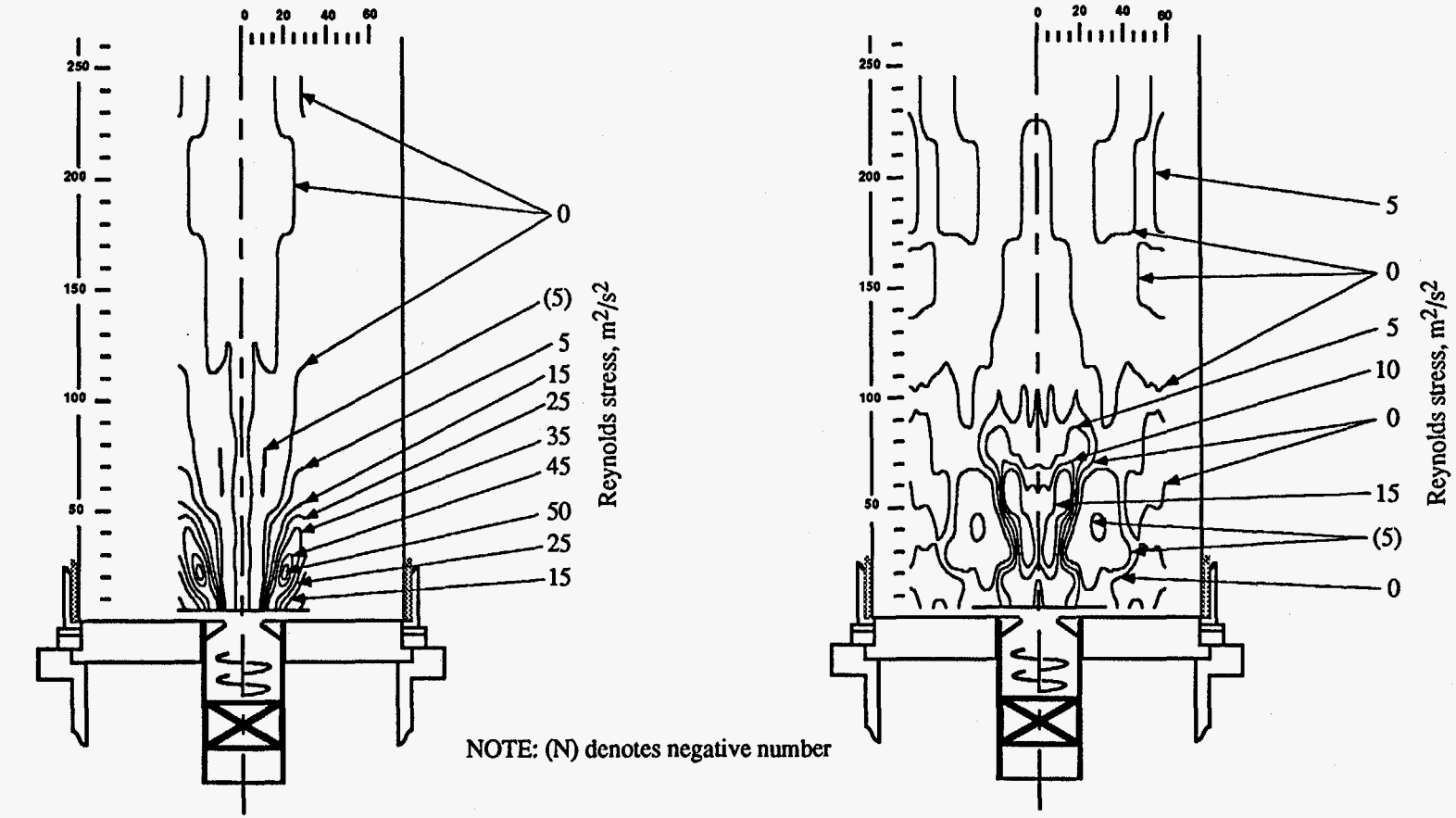

A) Axial-radial Reynolds stress $\phi = 0.65$

B) Axial-tangential Reynolds stress $\phi = 0.65$

Figure 3. Sample axial-radial $\overline{u'v'}$ and axial-tangential $\overline{u'w'}$ Reynolds stress contours for the ATS-MS burner at $\phi = 0.65$.

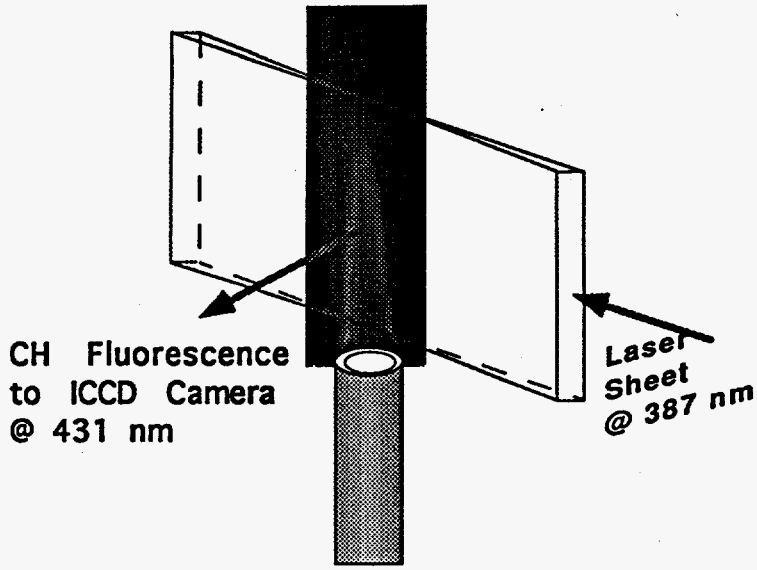

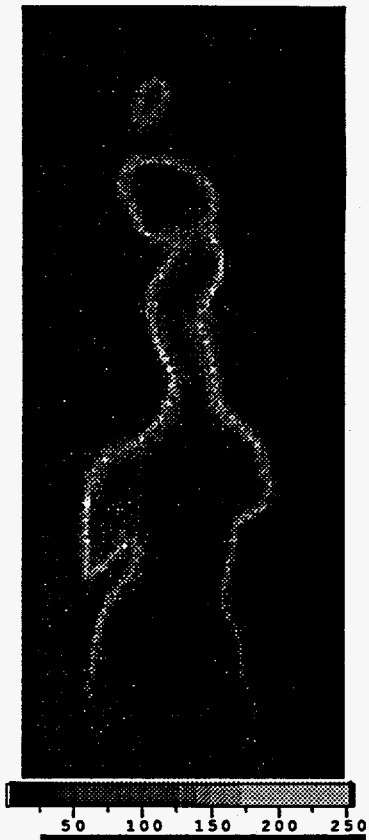

Figure 4

Above: Natural flame emission taken from video of natural gas bunsen burner.

Right/Below: Instantaneous bunsen burner CH fluorescence (F @ 1.0).

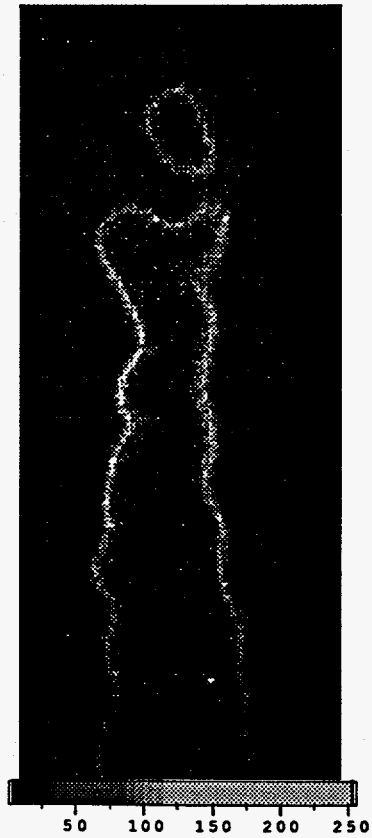

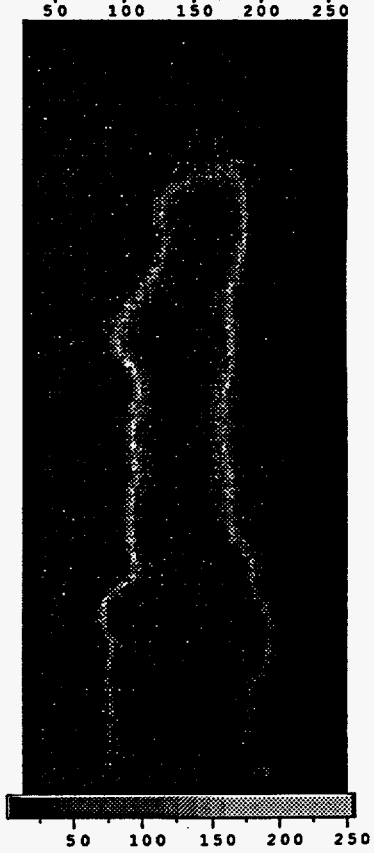

Bilger (Chen and Dibble, 1991). The reduced mechanisms were tested and compared against a full mechanism (GRI Mech. 1.2) for different conditions such as varying equivalence ratios, inlet temperatures, residence times, and pressures. A Perfectly-Stirred Reactor code (PSR) (Glarborg, et al., 1992) and a Premixed code (Kee, et al. 1992) were used to perform the evaluations. Efforts are also being made to acquire additional reduced mechanisms of methane combustion and the NOx mechanism which is in the being developed by GRI.

PSR code calculations: A total of 243 test calculations were performed using the PSR code in conjunction with the full mechanism and both reduced mechanisms, varying such parameters as pressure, equivalence ratios, inlet temperature, and residence time. In order to do these runs, the CHEMKIN package, which handles finite rate elementary reactions, had to be modified so that it could treat global reaction rates. The CKWYP subroutine in the package was replaced by a new subroutine which allowed calculation of global reaction rates.

The net rate constants for each of these global reactions are computed from algebraic expressions involving rate constants for about 25 elementary reaction steps. Figure 5 shows the variation of temperature with equivalence ratio for pressures of 1.0 and 30 atmospheres. The inlet temperature for the PSR reactor was taken as 600 K and the residence time was taken as 2×10^{-3} seconds. It is seen from Figure 5 that the Seshadri-Peters mechanism shows fairly good agreement with the full mechanism (GRI) at both pressures. The Bilger mechanism seems to show slight disagreement with the full mechanism (GRI) at high pressures for low equivalence ratios.

Figure 6 shows the CH_4 predictions for pressures of one and 30 atmospheres using the PSR code. It is seen that, although the Seshadri-Peters mechanism gives good predictions at 1 and 30 atm pressures, the Bilger mechanism gives poor predictions at both pressures for fuel-lean mixtures. Figure 7 shows the PSR CO predictions for the Peters-Seshadri, Bilger, and GRI full mechanism for pressures of 1 and 30 atm. It is seen that at both pressures, the two reduced mechanisms give almost identical predictions but differ from the full GRI mechanism predictions. It is postulated that the reduced mechanism predictions are more accurate at high pressure than at atmospheric pressure because C_2 chemistry is not included.

Premixed code calculations: The premixed code also runs in conjunction with the CHEMKIN package like the PSR, but is used to model burner-stabilized or freely propagating, steady-state, premixed laminar flames. Predictions of premixed laminar methane-air flames were performed using the full and reduced mechanisms as a function of pressure and equivalence ratio, using an inlet temperature of 300 K. Figure 8 shows the variation of temperature along the length of the premixed flow reactor for pressures of 1 and 30 atm (ϕ = 0.85). The Seshadri-Peters mechanism gives good agreement with the full mechanism at all pressures. Figure 9 shows CH_4 predictions using the premixed code for an inlet temperature of 300 K and an equivalence ratio of 0.85. The figure shows that at all pressures the combustion rate predicted by the full GRI mechanism is similar to the Seshadri and Peters reduced mechanism. Figure 10 shows the variation of predicted CO concentration with distance along the reactor for both 1 and 30 atm. The predictions show that the peak CO concentration in the Seshadri-Peters mechanism is slightly different compared to the full GRI mechanism (compare scales on the y axis).

Task 2 - Code Development

The objective of Task 2 is to develop an advanced, 3-dimensional gas turbine combustor model from the foundation of ACERC's existing 3-D code, PCGC-3. Task 2 is closely coordinated with an independently funded DOE/METC (DE-AC21-93MC30040) study being jointly conducted by Advanced Fuel Research, Inc. (AFR), and BYU/ACERC, which has a task for conducting gaseous combustion modeling.

2.1 - CFD Improvements. The objective of this subtask is to investigate improvements to the PCGC-3 fluid mechanics platform in order to better model the conditions and geometries associated with gas turbine

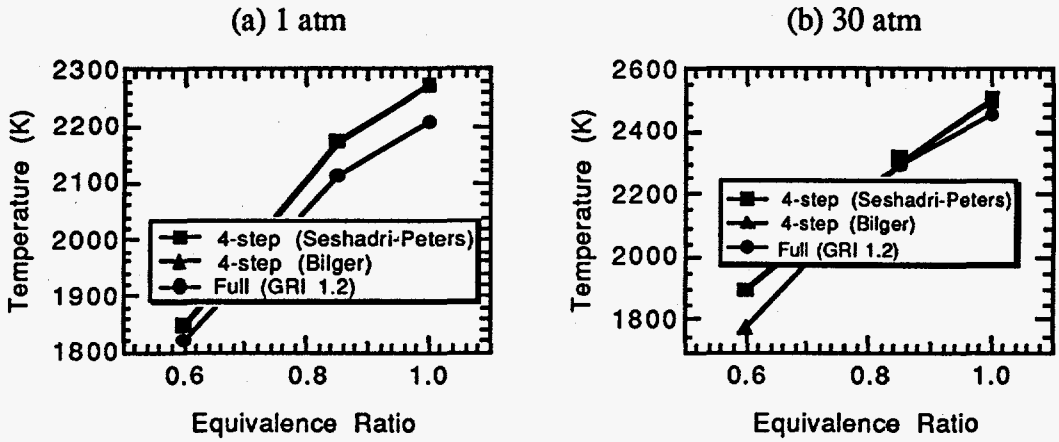

Figure 5. PSR calculations as a function of temperature and equivalence ratio (T_{inlet} = 600 K; τ = 2 ms)

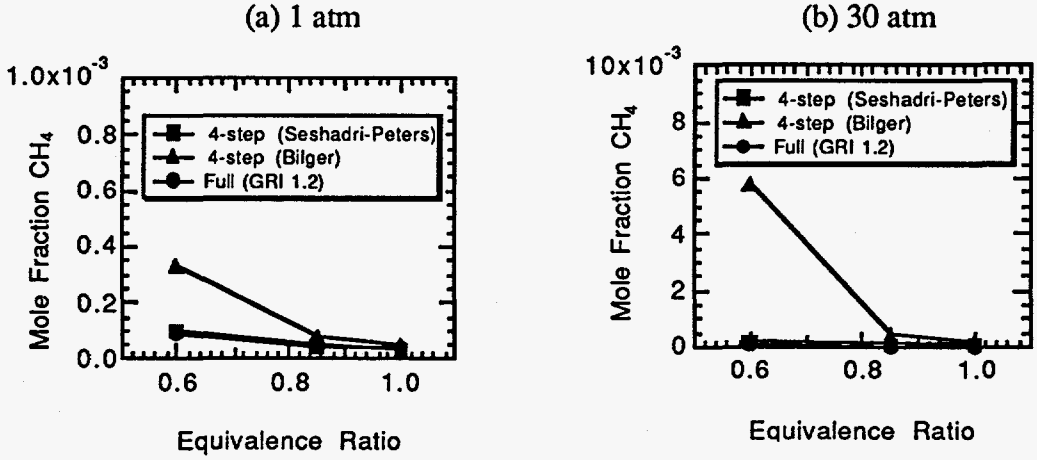

Figure 6. PSR calculations of mole fraction CH_4 as a function of equivalence ratio at two pressures (T_{inlet} =600 K; τ = 2 ms).

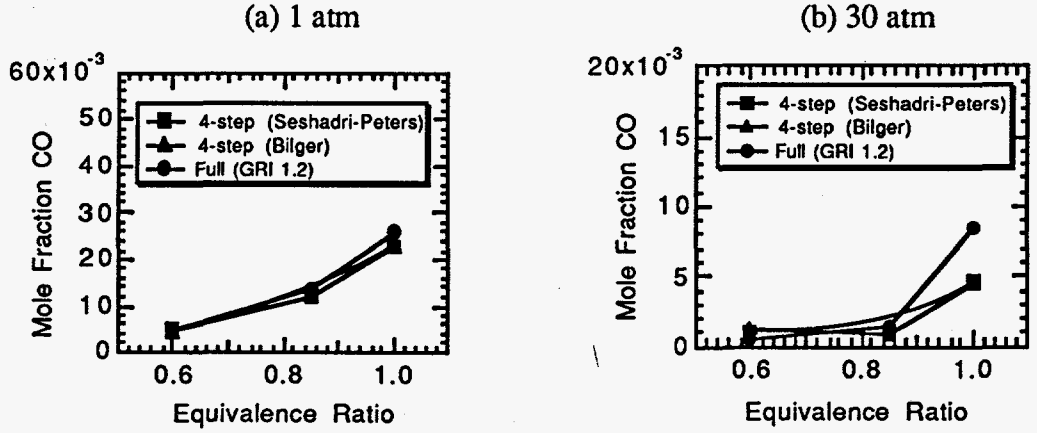

Figure 7. PSR calculations of mol fraction CO as a function of equivalence ratio at 1 and 30 atm (T_{inlet} =600 K; τ = 2 ms)

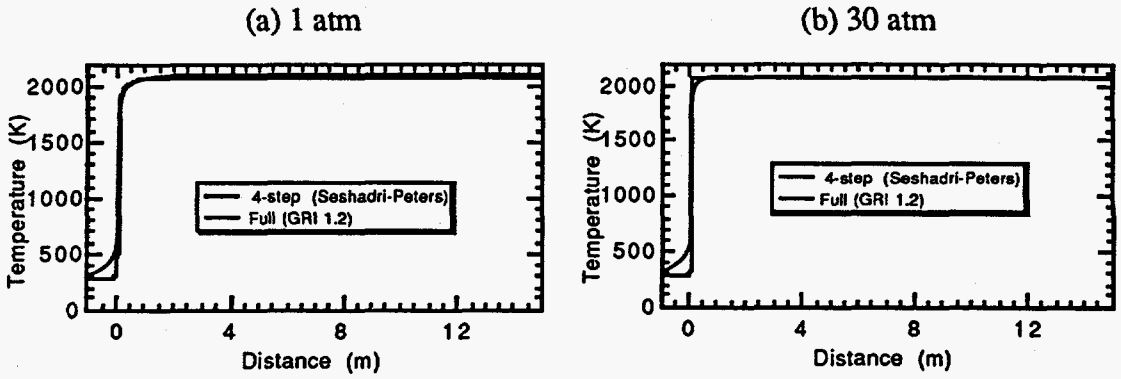

Figure 8. Premixed calculations of temperature (T_{inlet} = 300 K and ϕ = 0.85)

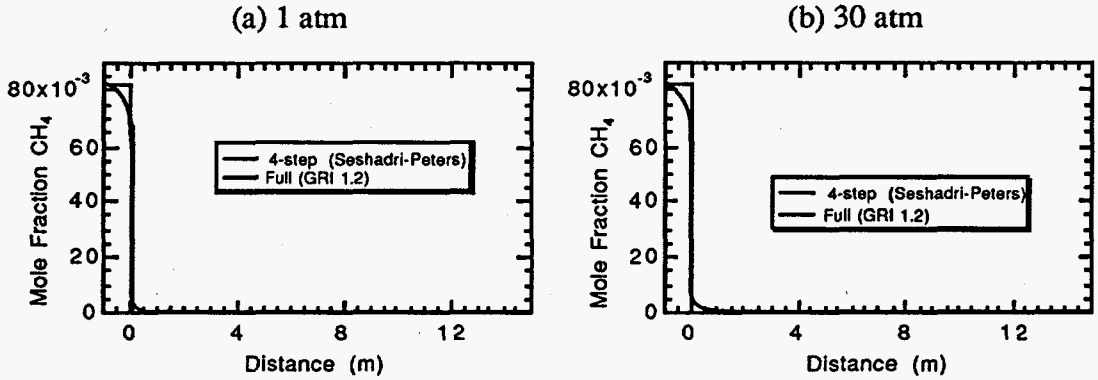

Figure 9. Premixed calculations of mole fraction CH_4 (T_{inlet} = 300 K, and ϕ = 0.85)

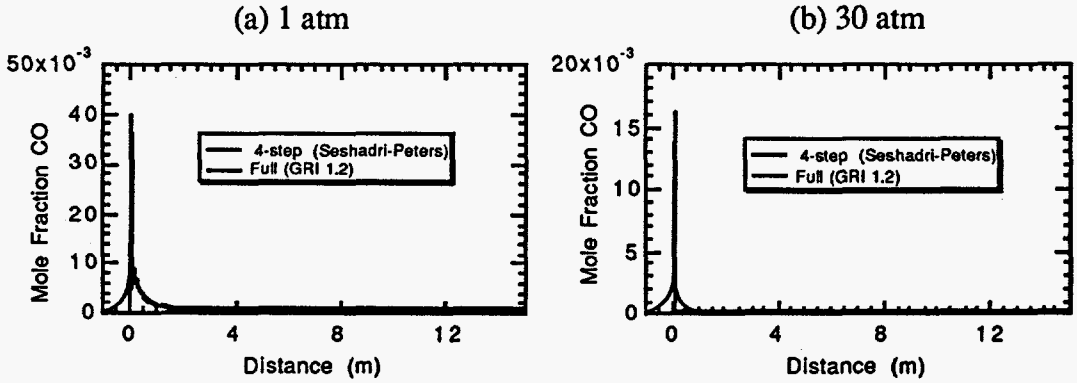

Figure 10. Premixed calculations of mole fraction CO (T_{inlet} = 300 K, ϕ = 0.85)

combustors. During the last year, the foundations of a new unstructured-grid flow solver were developed, under independent funding from the National Science Foundation (NSF), and the resulting code is being used as a basis for developing the gas turbine combustor model. The code uses the Control Volume Finite Element Method (CVFEM) of Baliga and Patankar (1983). Both collocated (Prakash, 1986) and staggered (Meng, 1994) schemes are employed. However, only the collocated scheme is operational at present. The skewed, mass-weighted upwind interpolation function for the dependent variables is used in the convection discretization, and linear interpolation functions are used for the diffusion, pressure gradient and source term discretization.

The new code was tested by simulating 1) developing laminar flow through a straight channel, 2) two-dimensional, laminar flow over a backward-facing step, and 3) turbulent flow over a backward-facing step. Calculations were also performed with FLUENT/UNS (Fluent Inc.'s unstructured-grid code) for comparison, and results were compared with experimental data or, in the case of laminar flow through the straight channel, with an analytical solution. Agreement was excellent for all of the laminar predictions. Geometry and predictions for turbulent flow over a backward-facing step are shown in Figure 11. Flat profiles were assumed at the inlet (x=-0.254 m), and the inlet turbulence intensity was assumed to be 5 percent. The grids were generated by GEOMESH (Fluent Inc.'s unstructured grid generator). The profiles have been normalized by the maximum velocity at each axial position. Experimental profiles were normalized by the maximum experimental velocity, and predicted profiles were normalized by the maximum predicted velocity. Raw data, without normalization, were not plotted because the experimental values were only available in normalized form. The predictions with two grid densities are similar, indicating that the solution is fairly grid-independent. The recirculation zone is significantly underpredicted, and the predicted velocity does not approach zero at the walls. Nodes that reside on the wall do not satisfy the no-slip condition. The manner of implementing the law-of-the-wall boundary condition is therefore being investigated to remedy this problem. Except for the near-wall regions, the shapes of the experimental and predicted profiles seem to be in reasonable agreement.

2.2 - Incorporation of Submodels. The objectives of this subtask are: 1) to incorporate the best-available, proven, advanced code submodels from the broad, on-going ACERC research program, from the literature, from known developers of submodels, and those developed in Task 1, and 2) to perform systematic checks of the code to verify accuracy of code programming, and appropriateness of newly installed improved submodels.

Implementation of PDF2DS into PCGC-3. An advanced gas-phase combustion submodel applicable to lean, premixed combustion (LPC) of natural gas in gas turbines is being developed under the independently funded DOE/METC project (DE-AC21-93MC30040). Such combustion is of significant commercial interest and yet there are no generally available combustion codes for predicting LPC flames. The submodel is intended for use in the comprehensive combustion code being developed under this study. The foundation of the submodel is PDF2DS, a 2-dimensional (2-D), velocity-scalar probability density function (PDF) code developed by Dr. Stephen Pope at Cornell University (Correa and Pope, 1992). Details of the velocity-scalar PDF method are given in Pope (1985). The submodel is being implemented under the independently funded study in PCGC-3.

The PDF2DS code has been implemented as a submodel in the 2-D, axisymmetric option of PCGC-3, and it has been tested for variable density, non-reacting flow. PCGC-3 calculates the flowfield, based on the k-e turbulence model, and PDF2DS calculates the density field. The two codes are coupled, as shown in Figure 12, and must be solved iteratively until the density field is no longer changing significantly in PDF2DS. The combined code seems to function reasonably well, except there is an inconsistency between

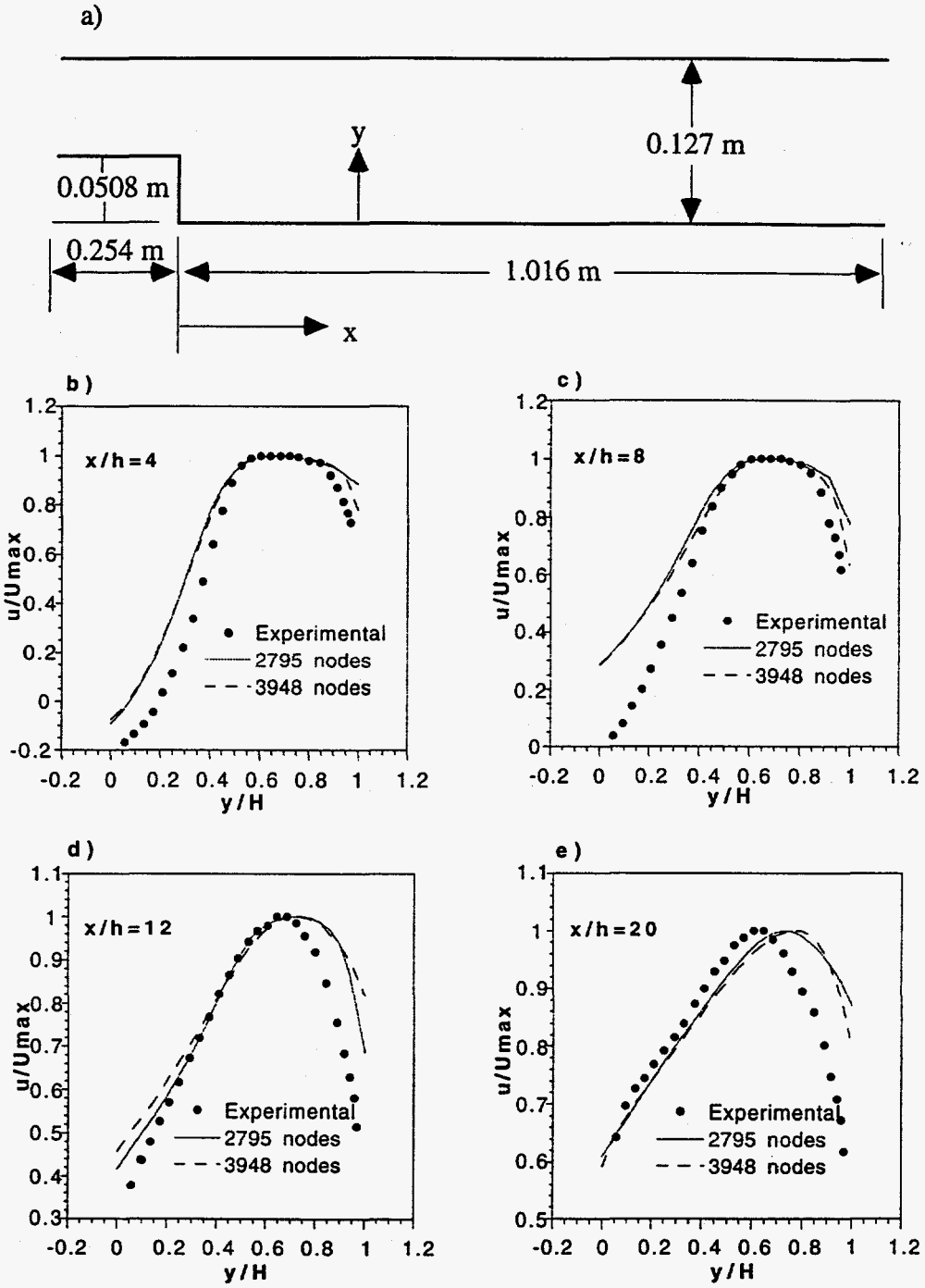

Figure 11. Geometry and predictions of axial velocity profiles for turbulent flow over a backward-facing step. (Experimental data from Westphal et al., 1984)

the computational grids of the two codes that seems to be causing problems. PCGC-3 uses a staggered grid, with velocities stored at cell faces and all other properties stored at cell centers, while PDF2DS uses a collocated grid with all properties stored at cell corners. Currently, PCGC-3 values are interpolated to the cell corners for use in PDF2DS and density is interpolated to the cell centers for use in PCGC-3. Consistency in grid definition is needed for the two codes to work compatibly.

Since PDF2DS provides no chemistry for reacting flow, the submodel is being extended to include chemistry applicable to LPC of methane, and table look-up procedures are being investigated to increase computational efficiency. A two-step mechanism (Westbrook and Dryer, 1981) is being implemented first. Later, a four-step mechanism (Seshadri and Peters, 1990) will be implemented.

Figure 13 shows a scatterplot of PDF particles for LPC of a methane-air jet with the two-step mechanism. Particle temperature is indicated by the shading, with the darkest particles at 300 K and the lightest (almost white) particles at 2012 K. The diameter of the jet was 2 cm, the equivalence ratio was 0.8, the inlet temperature was 300 K, and the jet Reynolds number was 36,140. The jet issued into a large cylindrical enclosure (1 m length, 0.4 m diameter). Radiation and heat losses were neglected. Approximately 100,000 PDF particles were used. Chemistry was implemented with the look-up tables described above.

Figure 14 shows a plot of CO mole fraction for particles residing in the first row of computational cells along the reactor centerline. Mole fractions exceeding equilibrium values were obtained at axial locations up to half the reactor length. Beyond this location, only equilibrium values were obtained.

Incorporation of PDF methods into the ACERC Unstructured-Grid Flow Solver. During the last year, integration of the advanced submodel applicable to LPC in gas turbines into the new unstructured-grid flow solver was performed and testing was initiated. An axisymmetric, constant-density, turbulent, non-premixed, non-reacting, test problem was solved as follows: First, the flowfield was converged by the flow solver (314 nodes, 550 cells). This step required approximately 500 iterations, starting from scratch (less than 30 CPU-min on an HP-735 workstation). Second, the PDF particles (91,146 total) were randomly distributed throughout the flow domain and initialized by linearly interpolating the velocity, pressure and turbulent kinetic energy from the unstructured mesh nodes onto the particle positions. Third, velocity-scalar PDF transport calculations were performed for the particles for 923 time steps (108 μsec/step), which is equivalent to approximately 10 reactor residence times. The PDF submodel calculations required approximately 14 CPU-hr (~1 CPU-min/time step). And finally, the mean mixture fraction field was calculated from the PDF particle mixture fractions using spline interpolation. Since the fluid mass density was uniform, there was no feedback from the PDF submodel to the flow solver. The predicted scalar mixing shows some unusual structural features (e.g., waviness) that are probably not realistic. This is probably due to the procedures that are used to interpolate grid properties on to the particles and/or visa versa. This issue is being investigated.

Incorporation of LPDF2D into PCGC-3. An updated version of a two-dimensional, node-based, scalar-only version of a probability density function (PDF) submodel, called LPDF2D, available from the NASA/Lewis Research Center, and which allows for the incorporation of gas-phase chemistry necessary for premixed combustion with turbulence interactions, was also obtained and incorporated into the axisymmetric option of PCGC-3 and tested. The advantage of the scalar-only PDF method is that it is simpler than the velocity-scalar method. The disadvantage is that it assumes gradient diffusion with a turbulent diffusivity. In LPDF2D, there is randomness in the implementation of both convection and diffusion. In PDF2DS, on the other hand, there is no randomness in the transport (by the mean and fluctuating velocity), i.e., the randomness is one level removed—in the fluid particle acceleration. Hence, the PDF method implemented in PDF2DS is more accurate than

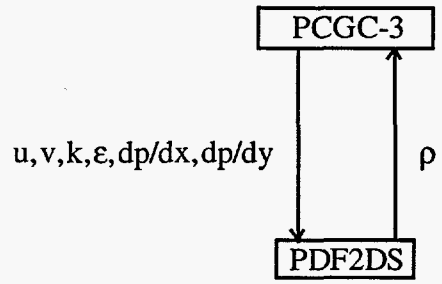

Figure 12. Coupling between PCGC-3 and PDF2DS.

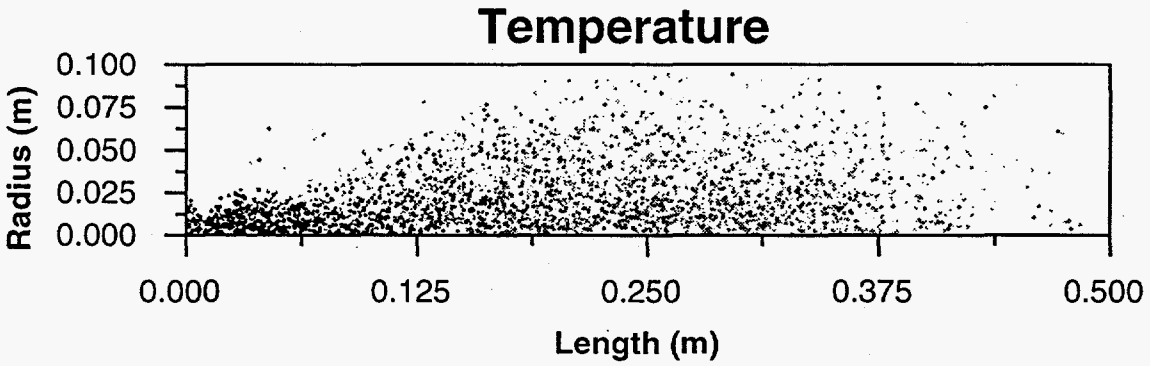

Figure 13. Scatterplot of PDF particle temperature in LPC of a methane-air jet.

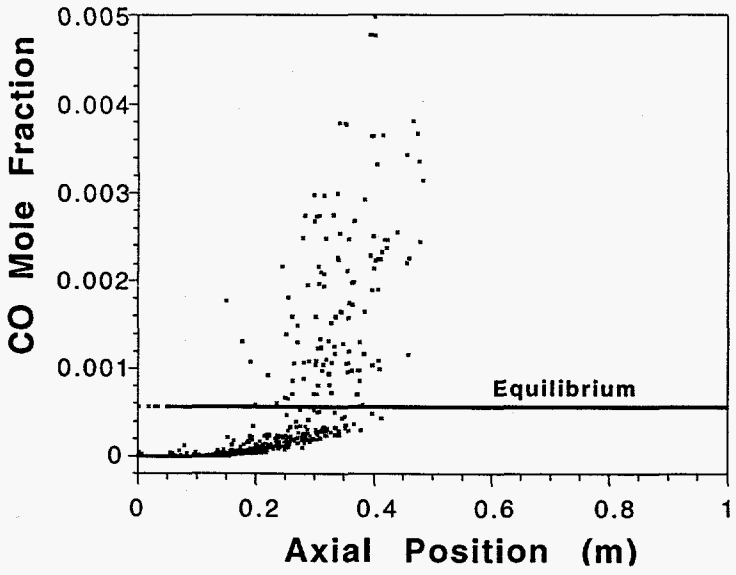

Figure 14. Predicted mole fraction of CO for PDF particles near the centerline of a premixed, methane-air jet.

that implemented in LPDF2D. Unfortunately, acceptable results were not obtained with LPDF2D, even for non-reacting flow. Several technical limitations were identified in the submodel and conveyed to researchers at NASA/LeRC. However, an improved version of the submodel, incorporating changes to address these limitations, is not yet available.

Subtask 2.3 - Parametric Predictions. The code is being used to make parametric predictions on advanced gas turbine designs obtained from the affiliated industrial manufacturers of gas turbine systems. Two practical gas turbine geometries were obtained from Westinghouse Electric Corp. Both are for premixers. The files for these geometries were created at Westinghouse by Computer Vision, a computer-aided design program, and transferred over the Internet in standard IGES format. The files were read at BYU by Fluent Inc.'s GEOMESH program, and boundary-fitted coordinate (BFC) grids were generated. Preliminary simulations with the FLUENT program (version 4.31) were then carried out to establish a methodology of generating computational grids based on solid modeling databases generated by design groups in industry. Simulation of the premixer shown in Figure 15a was then performed with the new ACERC code. Inlet conditions consisted of a low-velocity secondary inlet (air) and a high-velocity primary inlet (CH_4 at the small hole). Figure 15b shows the predicted scalar mixing (primary = 1, secondary = 0), on a cutting plane which sits perpendicular to the plane of the secondary inlet. The simulation results predict extensive, but not complete mixing of the fuel and oxidizer streams at the outlet.

Task 3 - Industry and AGTSR Interaction

The third task is to interact with industrial and university organizations with gas turbine interest. An ACERC/ATS technical advisory committee (TAC), composed of sixteen prominent industrial organizations with specific interest in utility and industrial gas turbine manufacture and application, was formed previously. The TAC provides direction for this research program. Concerns particular to industry are being addressed, and results are being provided to participating industrial members.

Members of the TAC have been contacted by telephone and mail, and have been sent copies of the annual report. The ASME Cogen Turbo Power conference was attended and the issues that were thought to be of most interest to the end user were discussed, such as combustor can burnout, restricted levels of turn-down, combustion stability problems, and NOx attainment when other fuels. There has been extensive interaction with Westinghouse and NASA-Lewis on geometries and modeling approaches. BYU investigators presented their work at the annual ATS program review at the ATS combustion workshop in Indianapolis. Visits to BYU have been made by Dr. J. Y. Chen (University of California, Berkeley) and Dr. Phillip C. Malte (University of Washington) to interact with the ATS program. A letter detailing the status of the project and asking for input from the members of the Technical Advisory Committee was recently sent.

In addition to the work being performed under this contract, research at BYU on advanced gas combustion models is being supported by other funding. The Department of Energy, through the Morgantown Energy Technology Center, is funding a collaborative project by Advanced Fuel Research (AFR) of East Hartford, CT, and BYU (contract number DE-AC21-93MC30040) which focuses specifically on the development of advanced submodels for turbulent, gaseous combustion. This study is referred to in this report as the AFR study. Further, ACERC is supporting several initiatives in adapting PCGC-3 to complex geometries and turbulence that complement work on this project. Other work has also been performed by ACERC researchers that can be applied to this project.

Future Activities

Task 1. Further velocity data will be acquired with natural gas as fuel for the MS configuration at $\phi = 1.2$, as noted above, and at $\phi = 0.65$, $\phi = 0.80$ $\phi = 1.0$, and $\phi = 1.2$ for the HS and LS configurations. In addition, LDA measurements will be taken for all three

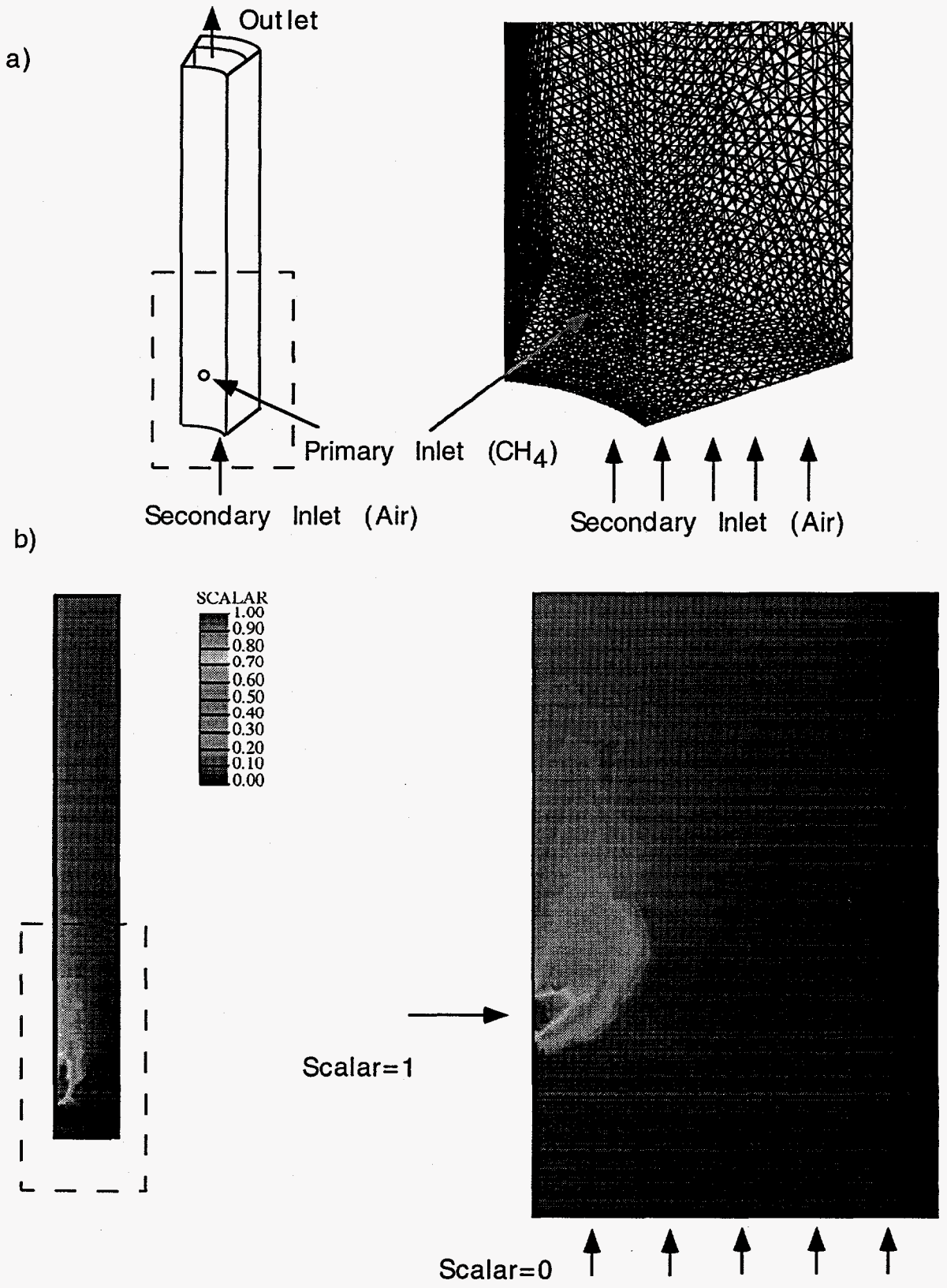

Figure 15. Geometry, computational grid and predicted scalar mixing for Westinghouse gas turbine premixer.

configurations (HS, MS, LS) with liquid ethanol as fuel. Again fuel equivalence ratios of ϕ = 0.80, ϕ = 1.0, and ϕ = 1.2 will be studied but ϕ = 0.65 will be replaced with a lean blowout condition, probably around ϕ = 0.50. Mapping of velocity, temperature, and N_2, O_2, CO, and CO_2 species concentrations for various configurations of the ATS premixed natural gas/air burner using LDA and CARS will be completed. In addition, PLIF images of OH and CH in the burner will be obtained.

Task 2. The ACERC unstructured code will be extensively revised and rewritten to improve accuracy, computational efficiency, and robustness. The unstructured-grid PDF submodel will be extended to variable-density, reacting flow and interfaced with a chemistry submodel for LPC being developed by an independently funded project. Both submodels will be incorporated in the unstructured-grid flow solver. Simulation of practical gas turbine combustor geometries will continue. One or more practical combustor "basket" geometries will be obtained from Westinghouse and simulated.

Future simulation efforts with the unstructured-grid code will focus on combustor "basket" geometries with chemical reaction. Because the inlet conditions and degree of premixing are so critical to predicting pollutant formation in LPC, non-reacting simulations of the premixer will be used to provide the inlet conditions for the combustor simulations. It is anticipated that the first reacting, combustor simulation for a practical geometry will be completed with the new unstructured-grid code and PDF submodel with kinetics for LPC on or around January 1, 1996.

Acknowledgments

This report was prepared with the support of the U.S. Department of Energy, Morgantown Energy Technology Center, Cooperative Agreement No. DE-FC21-92MC29061 (Dr. Paul Mitchell and Dr. Norm Holcombe, project managers). This financial support through the South Carolina Energy Research and Development Center, subcontract 93-01-SR014 (Mr. Daniel Fant, Program Director, and Dr. Lawrence P. Golan, SCERDC Director) is greatly appreciated. References are made in this report to work performed under separate funding agreements with the Advanced Combustion Engineering Research Center (with the principal grant from the National Science Foundation's Engineering Centers Division), Brigham Young University, the Air Force, and the DOE/METC with Advanced Fuel Research, Inc. Their support is appreciated. Students who participate on this project include Steven Cannon, Robert Dawson, Jason Haslam, Kyle Kinghorn, Hemant Mallampalli, Robert Murray, and Craig Phillips. Post-doctoral associates who have contributed include Fanli Meng and James Farmer. Also, the participation on the Technical Advisory Committee for this project of Allison Engine Company, General Electric, Solar Turbine, United Technologies Research Center, Westinghouse Electric Corp., Babcock and Wilcox, Foster Wheeler, Electric Power Research Institute, Gas Research Institute, Los Angeles Department of Water and Power, and Sacramento Municipal Utility District is greatly appreciated.

References

Baliga, B. R., and Patankar, S. V., "A Control Volume Finite-Element Method for Two-Dimensional Fluid Flow and Heat Transfer," Numerical Heat Transfer, 6, pp. 245-261 (1983).

Chen, J.Y. and Dibble, R.W., "Applications of Reduced Chemical Mechanisms for Prediction of Turbulent Non-Premixed Methane Jet Flames," in Reduced Kinetic Mechanisms and Asymptotic Approximations for Methane-Air Flames, M.D. Smooke (Ed.), Springer-Verlag, pp. 193-226 (1991).

Glarborg, P., Kee, R.J., and Miller, J.A., "PSR: A Fortran Program for Modeling Well Stirred Reactors," Sandia Report, (1992).

Kee, R.J., Grcar, J.F., Smooke, M.D., and Miller, J.A., "A Fortran Program for Modeling Steady Laminar One-Dimensional Premixed Flames," Sandia Report, (1992).

Meng, F., "A Staggered Control Volume Finite Element Method for Turbulent Reacting Flows Coupled with Radiation," Ph.D. dissertation, University of Montreal, CA (1994).

Peters, N., "Reducing Mechanisms," in Reduced Kinetic Mechanisms and Asymptotic Approximations for Methane-Air Flames, M.D. Smooke (Ed.), Springer-Verlag, pp. 48-67 (1991).

Prakash, C., "An Improved Control Volume Finite-Element Method for Heat and Mass Transfer, and for Fluid Flow using Equal-Order Velocity-Pressure Interpolation," Numerical Heat Transfer, 9, pp. 253-276 (1986).

Seshadri, K., and Peters, N., "The Inner Structure of Methane-Air Flames." Comb. Flame., 81, pp. 96-118 (1990).

Smooke, M.D. and Giovangigli, V., "Formulation of the Premixed and Nonpremixed Test Problems," in Reduced Kinetic Mechanisms and Asymptotic Approximations for Methane-Air Flames, M.D. Smooke (Ed.), Springer-Verlag, pp. 1-28 (1991).

Westbrook, C.K., and Dryer, F., "Simplified Reaction Mechanisms for the Oxidation of Hydrocarbon Fuels in Flames," Comb. Sci. Tech., 27, pp. 31-43 (1981).

Westphal, R. V., Johnston, J. P., and Eaton, J. K., "Experimental Study of Flow Reattachment in a Single-Sided Sudden Expansion," NASA Contractor Report 3765, Stanford University, Report MD-41 (1984).